GROUND MOTION VARIABILITY IN THE PO PLAIN REGION

AUTHORS			REVIEW			APPROVAL		
NOM	DATE	VISA	NOM	DATE	VISA	NOM	DATE	VISA
Francesca PACOR Giovanni Lanzano Maria D'Amico Chiara Felicetta Lucia Luzi Rodolfo Puglia INGV – MI			John DOUGLAS					
			Philippe RENAULT					

DISSEMINATION: Authors;Steering Committee;Work Package leaders, Scientific Committee, Archiving.

Executive Summary

This work represents the final step of the research activities carried out in the Po Plain region (Northern Italy) concerning the selection and calibration of Ground Motion Prediction Equations (GMPEs), suitable for seismic hazard assessments.

In the previous deliverable (Pacor et al. 2013), a strong-motion dataset for Northern Italy was compiled (DBN2_B). It is composed by 1539 waveforms recorded in the period between the 1976 Friuli sequence and the 2012 Emilia sequence and it was used to calibrate new regional equations for the Northern Italy.

In this work, we exploit this dataset to investigate the sources of the ground-motion variability. At the aim, we separate the total residuals (R_{ij}) into different contributions related to the between-event (δB_j), the site-to-site ($\delta S2S$) and the event and site corrected single-station ($\delta W_{ij,o}$) terms and evaluate their variability. The aim is to provide elements to implement the 'non-ergodic' approach in the Probabilistic Seismic Hazard Analysis (PSHA). In particular, we apply the method proposed by Rodríguez-Marek et al. (2011), afterwards developed by Luzi et al. (2014) to evaluate the single-station sigma (ϕ_{ss}).

The single-station sigma for the Northern Italy has been calculated considering both the entire strong motion dataset of Northern Italy (DBN2_B) and a subset of events and waveforms relative to the Emilia seismic sequence(hereinafter DBN2_E), characterized by a single-path sigma.

Contents

INDEX

GROUND MOTION VARIABILITY IN THE PO PLAIN REGION

1. <u>Introduction</u>

More than 1500 waveforms were considered in previous report (Pacor et al. 2013) for the strong motion dataset of Northern Italy (DBN2_B), with the final goal of selecting and calibrating regional Ground Motion Prediction Equations (GMPEs).The bulk of DBN2_B is represented by the 2012 Emilia seismic sequence, recorded by national networks and temporary arrays installed after the mainshock (M 6.1), which occurred on 20 May 2012.

DBN2_B highlights some peculiar features in the Po Plain region, such as: i) low amplitudes at short periods; ii) attenuation with distance strongly dependent on frequency; iii) amplification of spectral ordinates in the distance range from 80 to 100km, particularly evident at short periods (0.1 s); iv) strong amplification at low frequencies for stations located on the deep sediments of the valley (Luzi et al. 2013).

DBN2_B was adopted for calibrating regional predictive equations, in which a new site class (C1) is introduced to represent the stations located inside the Po Plain that could be affected by 2D and 3D propagation effects. These GMPEs fit adequately the observations, although the total standard deviation (σ_{tot}) is rather high, varying between 0.74 and 0.94 (ln units), with the largest values observed at short periods.

The preliminary decomposition analysis of the total residuals,defined as the difference between the observations and the predicted values in logarithm scale, showed that:

1) the largest variability is associated to the within-event component, probably due to the large variation of the site response in the Po Plain valley and between rock sites located on the Alps and Appennines;

2) the site-to-site term is variable even for C1 sites, although they are expected to have similar geological features.

	Research and Development Program on Seismic Ground Motion	**Ref : SIGMA-2014-D2-133** **Version : 02**
EDF cea AREVA Enel Σigma L'ENERGIA CHE TI ASCOLTA. Seismic Ground Motion Assessment	CONFIDENTIAL *Restricted to SIGMA scientific partners and members of the consortium, please do not pass around*	**Date :** February 17th 2015 **Page :**6 / 42

In this study, the single station sigma, i.e. the ground motion variability after removing the contribution related to the repeatable effects of site response and seismic events, has been computed and discussed according to Rodriguez-Marek et al. (2013).

This deliverable has been organized as follows. First, we present the adopted methodology and the characteristics of the employed datasets; then we introduce the residual analysis and we evaluate the different contributions of the standard deviations. Finally, we discuss the site term and the single station sigma at representative sites, some of these selected for probabilistic hazard analysis.

2. <u>Methodology</u>

To investigate the possible causes of the uncertainties that are not captured by the GMPEs calibrated in the Po Plain (DBN2_B),we analyze the total residuals and we isolate the contributions related to the events, to the sites and to the random variability (Scasserra et al., 2009; Al Atik et al., 2010).

This is accomplished by decomposing the residuals according to the following expression:

$$R_{ij} = \delta B_i + \delta W_{ij} \qquad [1]$$

where the subscripts *i* and *j* refer to events and stations, respectively.

R_{ij} is computed as the difference between the logarithm of observation and prediction, δB_i represents the between-events residual (event-term), which corresponds to the average misfit of recordings of one particular earthquake with respect to the median ground-motion model; δW_{ij} represents the within-event residual, which corresponds to the difference between the residual and δB_i. Following the approach of Rodriguez-Mareket al. (2011) and Luzi et al. (2014), the within-event residuals are then exploited to evaluate the site-term for each station j:

$$\delta S2S_j = \frac{1}{NE_j}\sum_{i=1}^{NE_j}\delta W_{ij} \qquad\qquad [2]$$

where NE_j is the number of events recorded at the station j.

This term quantifies the average misfit of recordings from one particular site with respect to the event-corrected median ground-motion.

This is a zero mean random variable and its standard deviation is denoted by ϕ_{S2S}, which quantifies the variability from site to site, which cannot be explained by the model.

The within-event residual can be thus written as:

$$\delta W_{ij} = \delta S2S_j + \delta W_{o,ij} \qquad\qquad [3]$$

Where $\delta W_{o,ij}$ is the remaining residual after site and event terms are subtracted from total residuals.

The event-corrected single-station standard deviation at individual site can be computed as:

$$\phi_{ss,s} = \sqrt{\frac{\sum_{i=1}^{NE_j}\left(\delta W_{ij} - \delta S2S_j\right)^2}{NE_j - 1}} \qquad\qquad [4]$$

and the event-corrected single-station standard deviation of all stations is:

$$\phi_{ss} = \sqrt{\frac{\sum_{j=1}^{NS}\sum_{i=1}^{NE_j}\left(\delta W_{ij} - \delta S2S_s\right)^2}{\left(\sum_{j=1}^{NS}NE_j - 1\right)}}$$
[5]

Where *NS* is the number of stations in the dataset.

Finally, the total single-station standard deviation can be computed as:

$$\sigma_{ss} = \sqrt{\phi_{ss}^2 + \tau^2}$$
[6]

where τ is the between-event standard deviation.

Table 1 summarizes the components of the total residuals, the corresponding standard deviations and the adopted terminology.

Table1. Components of total residuals and standard deviations (Rodriguez-Marek et al., 2013).

Residual components	Notation	Standard deviation components	Notation
Total residual	$R_{ij} = \delta B_i + \delta W_{ij}$	Total standard deviation	$\sigma_T = \sqrt{\tau^2 + \phi^2}$
Between-event residual	δB_i	Between-event standard deviation	τ
Within-event residual	δW_{ij}	Within-event standard deviation	ϕ
Site term	$\delta S2S_j$	Site-to-site variability	ϕ_{s2s}
Event and site corrected residuals	$\delta W_{o,ij} = \delta W_{ij} - \delta S2S$	Event corrected Single-station standard deviation	ϕ_{ss}
		Event corrected Single-station standard deviation at individual site	$\phi_{ss,s}$
		Total Single-station standard deviation	$\sigma_{ss} = \sqrt{\phi_{ss}^2 + \tau^2}$
		Total Single-station standard deviation at individual site	$\sigma_{ss,s} = \sqrt{\phi_{ss,s}^2 + \tau^2}$

3. <u>Datasets</u>

The components of the variability of ground motion models in Northern Italy and in particular in Po Plain have been evaluated using two datasets.

1. Dataset DBN2_B: it was compiled in the first phase of the Project (Pacor et al., 2012; 2013) and used to derive the regional GMPEs for Northern Italy. The stations and events distribution is shown in Figure 1a. The dataset mainly includes the events of two main seismic sequences of 1976 (Friuli, M 6.4) and 2012 (Emilia, M 6.1); the latter provides a huge quantity of high quality strong-motion records and represents about the 2/3 of the entire dataset. In DBN2_B, the stations are mainly located within the Po plain, on the central and eastern Alps and on the sector of northern Apennines. The dataset has been obtained selecting records in the magnitude range 4.0 - 6.4; the distance range (Joyner and Boore distance or epicentral distance, when the first was not available) is 0-200km and the event depth is lower than 30km; four styles of faulting have been accounted for (Normal NF, Thrust TF-TS, Strike Slip SS, Unknown UN). The minimum number of recordings for each station is 3. No selection was done on number of records per earthquake. In summary, DBN2_B consists of 1539 records from 79 events and 173 stations (Table2).

2. Dataset DBN2_E: this dataset is composed only by the 2012 Emilia sequence events occurred in the time period 19th May 2012 -16th June 2012 within the spatial limits 10.6 – 11.7E/44.6 – 45.2N. The stations and events distribution is shown in Figure 1b. The majority of sites is within the Po plain and are located close to the epicentres, the farther ones are located on the border of the Alps and the Apennines with the Po plain. All the events have thrust style of faulting and shallow focal depths (< 15 km); the considered magnitude range is 4.0-6.1 and the maximum epicentral distance

is 200km. The minimum number of recordings of each station is 5. The number of recordings in DBN2_E is 937, relative to 22 events and 88 stations (Table 2).

The main characteristics of the two datasets are described in Table 2: in both datasets, the magnitude is moment magnitude, Mw if available, otherwise the local magnitude Ml, the distance is the Joyner and Boore distance if the source geometry is available (in total 4 events with M> 5.5), otherwise the epicentral distance
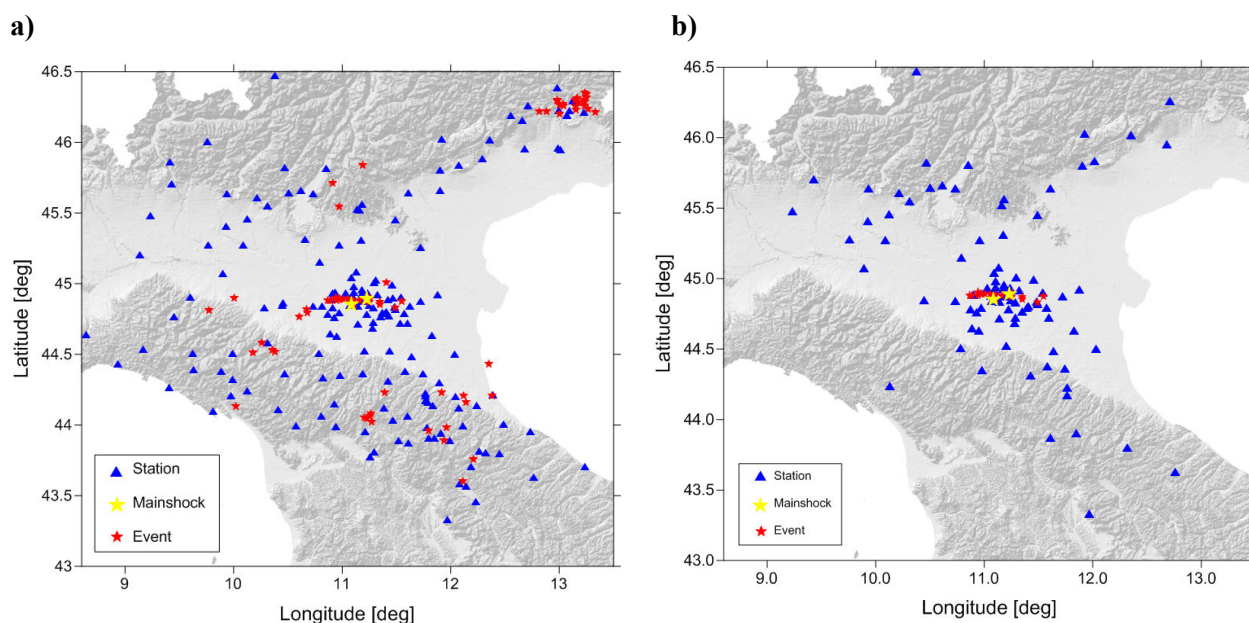
a)   b)

Figure 1: Location of stations (blue triangles) and events (red stars) of the DBN2_B (a) and DBN2_E (b) datasets. The main events of the 2012 Emilia sequence are depicted by yellow stars.

Table 2. Main features of the selected datasets.

Dataset	Rec	Eve	St	Rec/St.	Mw/Ml	R [km]	H [km]
DBN2_B	1539	79	173	≥ 3	4.0 − 6.4	0 - 200	30
DBN2_E	937	22	88	≥ 5	4.0 − 6.1	0 - 200	15

In both datasets, the recording sites are separated into 4 classes, based on the shear wave velocity intervals in the uppermost 30 m(V_{s30}) according to the EC8 classification (CEN, 2003) and on the position with respect to the Po Plain: class A: V_{s30}> 800 m/s; class B: V_{s30} = 360 − 800 m/s; class C: V_{s30} = 180 − 360 m/s, located outside or on the border of the plain; class C1:V_{s30} = 180 − 360 m/s, located within the plain. However, it is important to note that the majority of the sites has been

10

	Research and Development Program on Seismic Ground Motion	Ref : SIGMA-2014-D2-133 Version : 02
edf cea AREVA Enel L'ENERGIA CHE TI ASCOLTA. Σigma Seismic Ground Motion Assessment	CONFIDENTIAL *Restricted to SIGMA scientific partners and members of the consortium, please do not pass around*	**Date :** February 17th 2015 **Page :** 11 / 42

classified according to a geological description and only for about 35 sites, in-situ measures of $V_{S,30}$ are available. As shown in Table 3, the datasets are dominated by stations belonging to the C and C1 classes, providing about 60% and 80% of the records for DBN2_B and DBN2_E, respectevely. Classes A and B are sufficiently sampled in case of DBN2_B, both in terms of records and stations, while they are very few in case of DBN2_E.

Table 3. Number of records and stations per site class.

	Site A Rec/St	Site B Rec/St	Site C Rec/St	Site C1 Rec/St
DBN2_B	377/47	245/27	286/33	631/66
DBN2_E	188/18	103/9	146/12	500/49

The scatter-plot of the magnitude-distance distribution for DBN2_B and DBN2_E is reported in Figure 2a and 2b, distinguishing the data on the base of the soil categories. In both datasets the site classes are not uniformly distributed over distance: while the C and C1 sites are mainly located in epicentral area, the A and B sites are generally far from the seismic sources. This feature is particular evident for DBN2_E, only composed by strong motion data of the Emilia sequence, mainly recorded by stations belonging to the C1 class.

Figure 2c illustrates the data-distribution of DBN2_E dataset, compared to the DBN2_B one. The main difference is due to the records of the Friuli seismic sequence, that better sample the largest magnitudes (M> 6) and the distance range 80 – 100 km for magnitudes from 4 to 5.5.
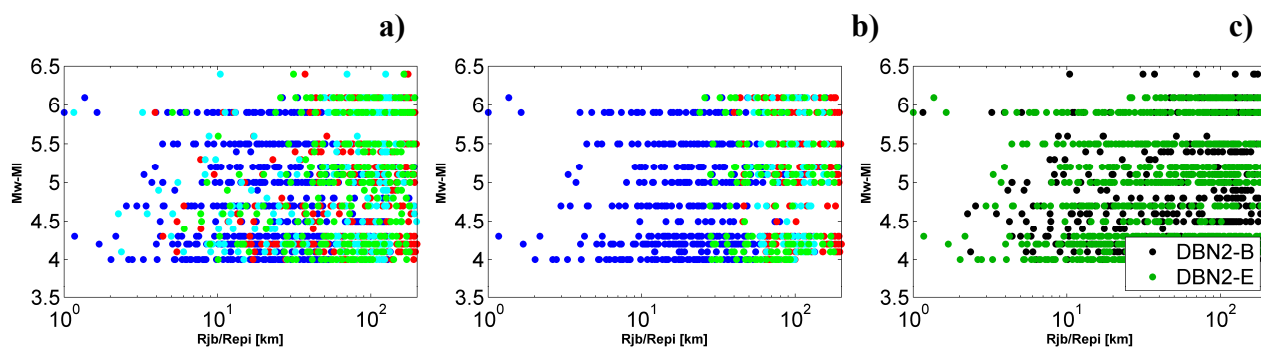

Figure 2. Distance-magnitude distributions for DBN2_B (a) and DBN2_E (b); the colors represent the site classes: A: red, B: light blue, C: green, C1: blue. Comparison between the two distributions (c).

Figure 3 shows the record-distributions in term of magnitudes, distances and hypocentral depths for the two datasets. The majority of strong motion data are relative to small events (M 4 - 4.5), recorded within 20km from the epicenters. These waveforms are mainly recorded by temporary stations and arrays installed in the epicentral area, immediately after the main shock of the Emilia sequence (20 May 2012), to monitoring the sequence and to investigate the site effects in the Po plain region.
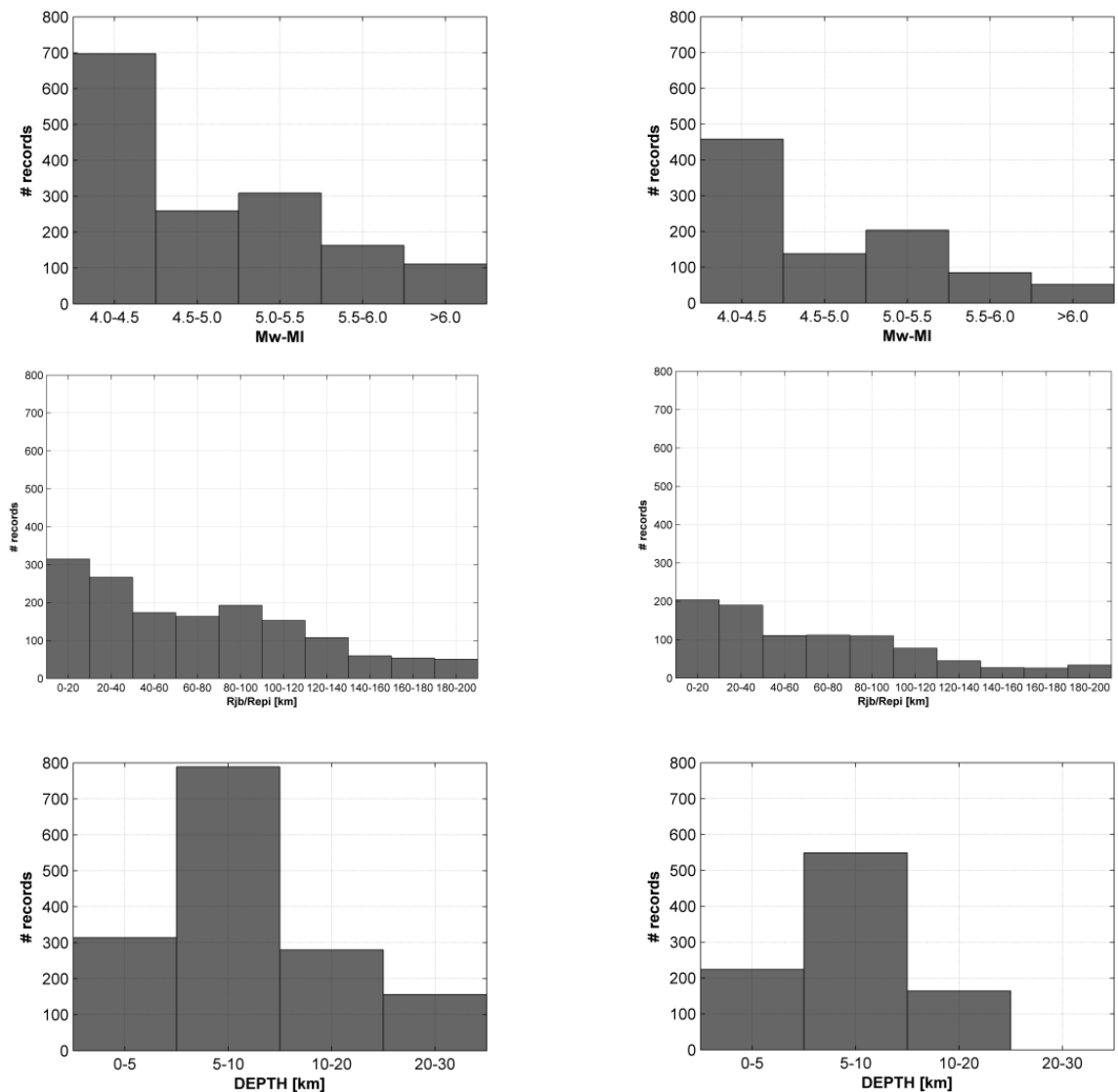

Figure 3. Strong-motion data distribution as a function of Magnitude, distances from the source (Joyner-Boore distance or epicentral distances) and focal depths. Left: DBN2_B.Right: DBN2_E.

	Research and Development Program on Seismic Ground Motion	**Ref : SIGMA-2014-D2-133** **Version : 02**
edf cea AREVA Enel ∑igma L'ENERGIA CHE TI ASCOLTA. Seismic Ground Motion Assessment	CONFIDENTIAL *Restricted to SIGMA scientific partners and members of the consortium, please do not pass around*	**Date :** February 17th 2015 **Page :** 13 / 42

The major contribution in terms of records comes from the 4 strongest Emilia events recorded by more than 100 stations within 200 km from the epicenters (Table 4).

Table 4. Earthquakes of the 2012 Po Plain sequence characterized by more than 100 strong-motion data (#recs), recorded within 200 km from the epicentre.

Event time	Lat	Lon	H [km]	M_w	# rec
20/05/2012 02:03:52	44.89	11.23	6.3	6.1	168
29/05/2012 07:00:03	44.85	11.09	10.2	5.9	158
29/05/2012 10:55:57	44.89	11.01	6.8	5.5	124
03/06/2012 19:20:43	44.90	10.94	9.2	5.0	116

The Emilia events have been densely sampled in epicentral area and the observations can be interpolated to have an overview of the variability of the ground motion in proximity of the source. As an example, Figure 4 shows the spatial distribution of the geometrical mean of the two horizontal components for the Peak Ground Acceleration (PGA) and Peak Ground Velocity (PGV) for some events of the Emilia sequence.

The waveforms have been processed uniformly, according to the procedure described in Paolucci et al. (2011): (1) baseline correction; (2) application of a cosine taper, based on the visual inspection of the record (typically between 2 and 5% of the total record length); records identified as late-triggered are not tapered; (3) visual inspection of the Fourier spectrum to select the band-pass frequency range; (4) application of a 2nd order a-causal time-domain Butterworth filter to the acceleration time-series padded with zeros; (5) double-integration to obtain displacement time series; (6) linear de-trending of displacement and (7) double-differentiation to get the corrected acceleration.
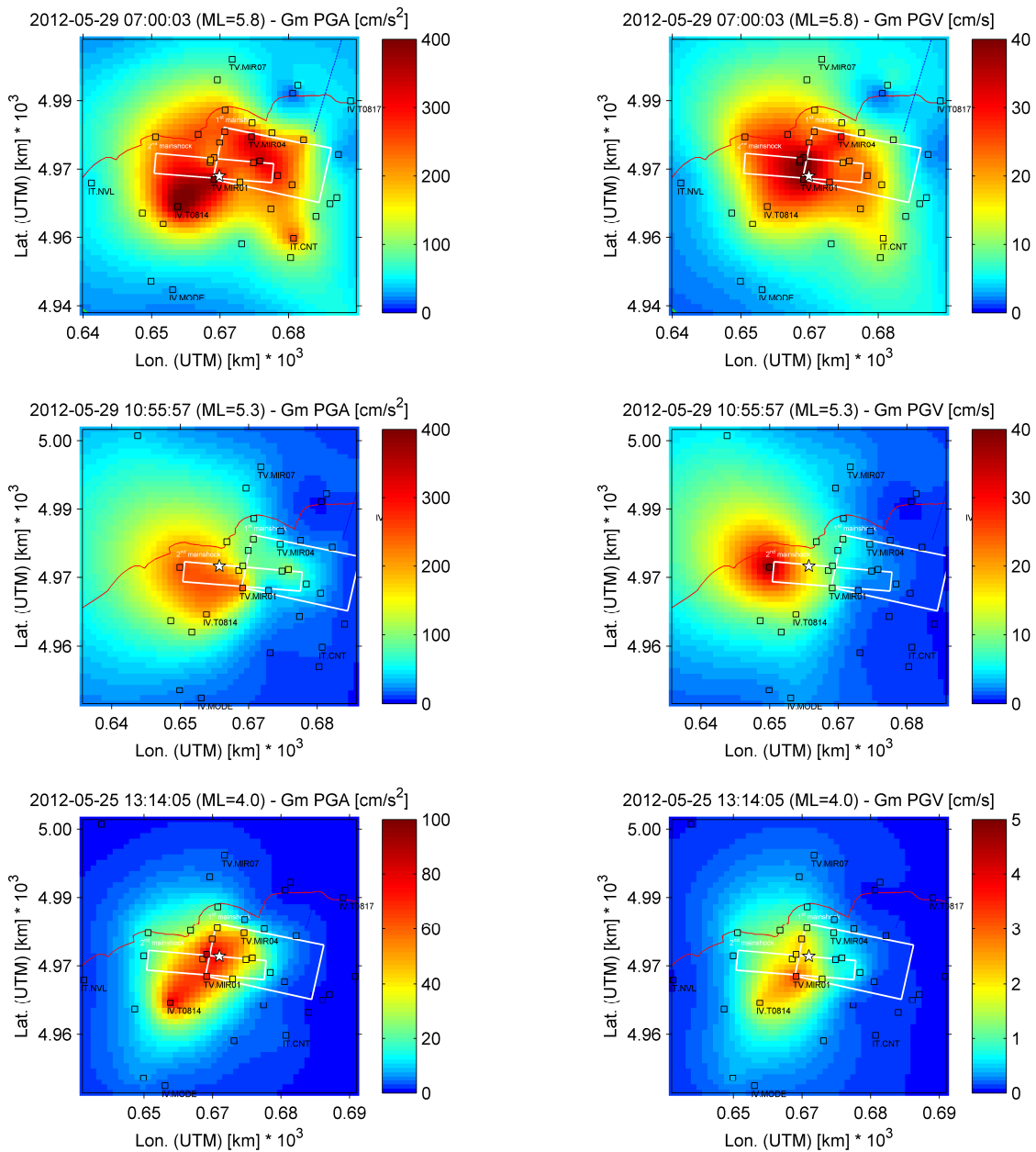
Figure 4. Maps of the interpolated ground motion parameters (geometric mean Gm of the horizontal components) for three events of the Emilia sequence. Left: PGA. right: PGV. The white rectangles represent the geometry of the two main events (20 May 2012 and 29 May 2012); the black squares are the recording stations; the white star is the epicenter.

	Research and Development Program on Seismic Ground Motion	Ref : SIGMA-2014-D2-133 Version : 02
edf cea AREVA **Enel** L'ENERGIA CHE TI ASCOLTA. **∑igma** Seismic Ground Motion Assessment	CONFIDENTIAL *Restricted to SIGMA scientific partners and members of the consortium,* *please do not pass around*	Date : February 17th2015 Page :15 / 42

4. <u>Residuals analysis</u>

In this section, for the two datasets DBN2_B and DBN2_E,we evaluate the residuals, the error components and the standard deviations for the geometric mean of the horizontal ground motion components.

The analysis is carried out considering the regional GMPEs (DBN2_GMPEs) calibrated in the previous steps of the project (Pacor et al., 2012; 2013); the functional form is the following (e.g. Bindi et al., 2011):

$$\log_{10} Y = e_1 + F_D(R,M) + F_M(M) + F_S + F_{sof} \qquad [6]$$

where the distance F_D and magnitude F_M functional forms are given by:

$$F_D(R,M) = \left[c_1 + c_2 \left(M - M_{ref} \right) \right] \log_{10} \left(\sqrt{R_{JB}^2 + h^2} \, / \, R_{ref} \right) - c_3 \left(\sqrt{R_{JB}^2 + h^2} - R_{ref} \right) \qquad [7]$$

$$F_M(M) = \begin{cases} b_1 \left(M - M_h \right) + b_2 \left(M - M_h \right)^2 & for\, M \le M_h \\ b_3 \left(M - M_h \right) & otherwise \end{cases} \qquad [8]$$

The explanatory variable M is the event-magnitude (moment magnitude or local magnitude), R(in km) is Joyner and Boore or epicentral distance; the dummy variables F_S ($F_S = s_i C_i$, for i=1,...4) and F_{sof} ($F_{sof} = f_j E_j$, for j=1,...4) in equation (6) represent the site amplification and the style of faulting terms, respectively. The variables M_{ref}, M_h, R_{ref} (equations 7 and 8) are fixed to 5.0, 6.75 and 1km, respectively, after trial regressions and after Bindi et al. (2011). In particular, M_{ref} was selected after analysing the decay with distance of observed peak values at different magnitudes (deliverable SIGMA0002, Pacor et al., 2013). Y is the predicted variable (PGA and the 5% PSA in the period range T=0.04 - 4s), obtained for the geometrical mean (GEOH) of the horizontal components.

The soil coefficients of the DBN2_GMPEs are shown in Figure 5 as a function of the period T. These coefficients show expected trends: class B (grey circles) has an amplitude peak of 0.25 around 0.3s;class C (black circles) amplifies the long period range after 0.3s; class C1 (white circles) causes a relevant amplification of long period ground motion, after 0.2s.
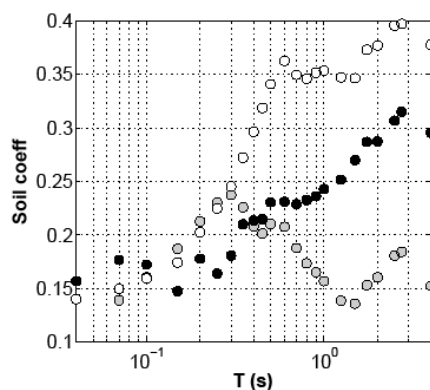

Figure 5. Site coefficients of GMPEs vs. period for the GEOH. White circle: C1 class; black circle: C class; grey circle: B class.

Total residual distributions

The total residuals R_{ij}, defined as the natural logarithm of the ratio between observations and predictions, are shown as a function of the distance in Figure 6 and 7; for both datasets the residuals are in the range -3/+3.

DBN2_B and DBN2_E residuals show a complex trend with distance, especially at short periods: they present two bumps centered on 10 and 100km, while negative values are observed in the range $30 - 60$ km (i.e. observations lower than predictions). Conversely, at longer periods the residuals show a weaker dependence on distance (Pacor et al. 2013).
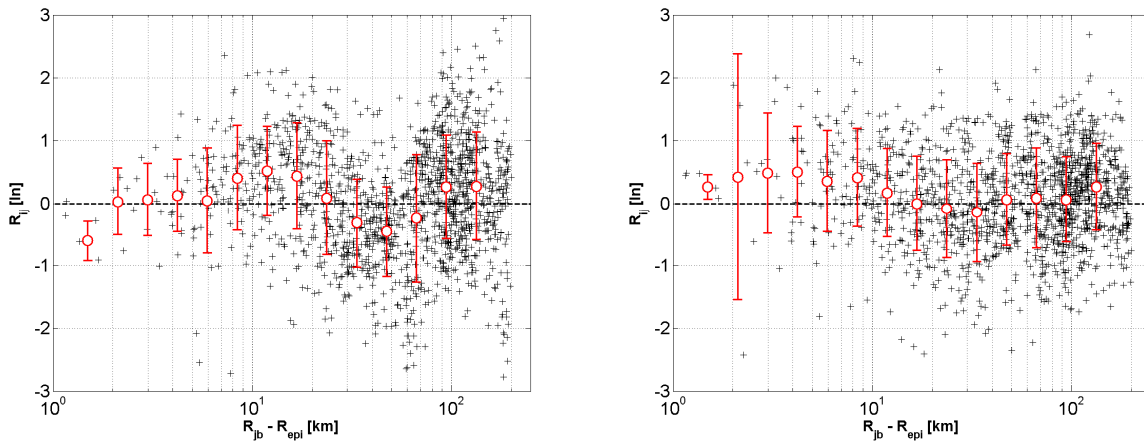
Figure 6. DBN2_B total residuals vs. distance computed as ln (observation/prediction). T= 0.1s (left) and 2.0s (right).

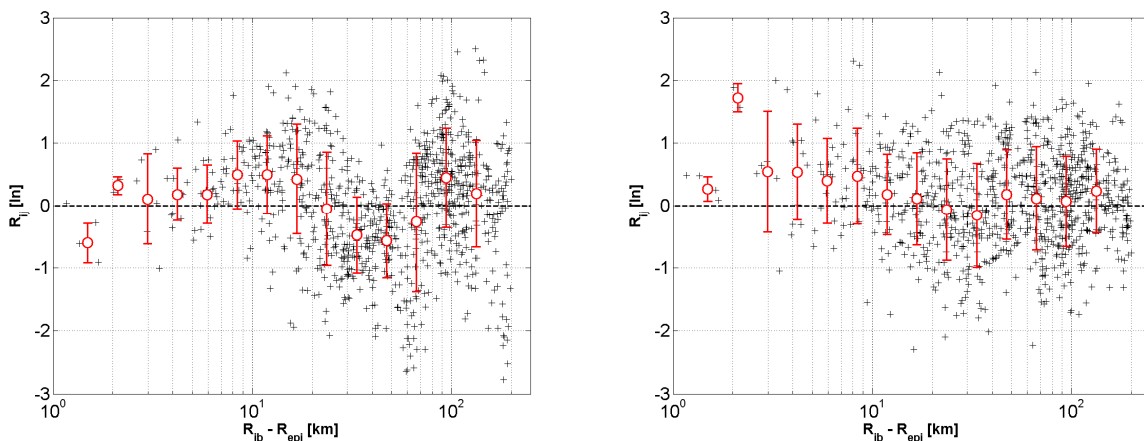**Figure 7.** DBN2_E total residuals vs. distance computed as ln (observation/prediction).T= 0.1s (left) and 2.0s (right).

To better understand the complex behavior of the residual distribution in Figure 6 and 7, the total

residual have been decomposed into its components, as described in section 2 and Table 1.

Event terms

In this study, for each event, the event-errors are estimated as the mean of the residuals. Figure 8

shows the distribution of the between-event errors of the DBN2_B and DBN2_E, at periods 0.1 and

2.0s. In these figures, the events are plotted in chronological order. ANNEX A reports for each

event the associated metadata and the between errors for all considered periods.

The between-event errors for DBN2_B vary in the range from −1.5 to 1.5 and they are generally positive. On the contrary, the DBN2_E errors vary in a smaller range (from −0.6 to 0.6) around zero. The largest errors are observed at short periods, in correspondence of the oldest events, probably due to the poor quality of associated metadata. Moreover these past earthquakes have been recorded by a small number of stations (mainly analogic instruments), biasing the value of the event-errors when estimated as the mean of the residuals relative to each earthquake.
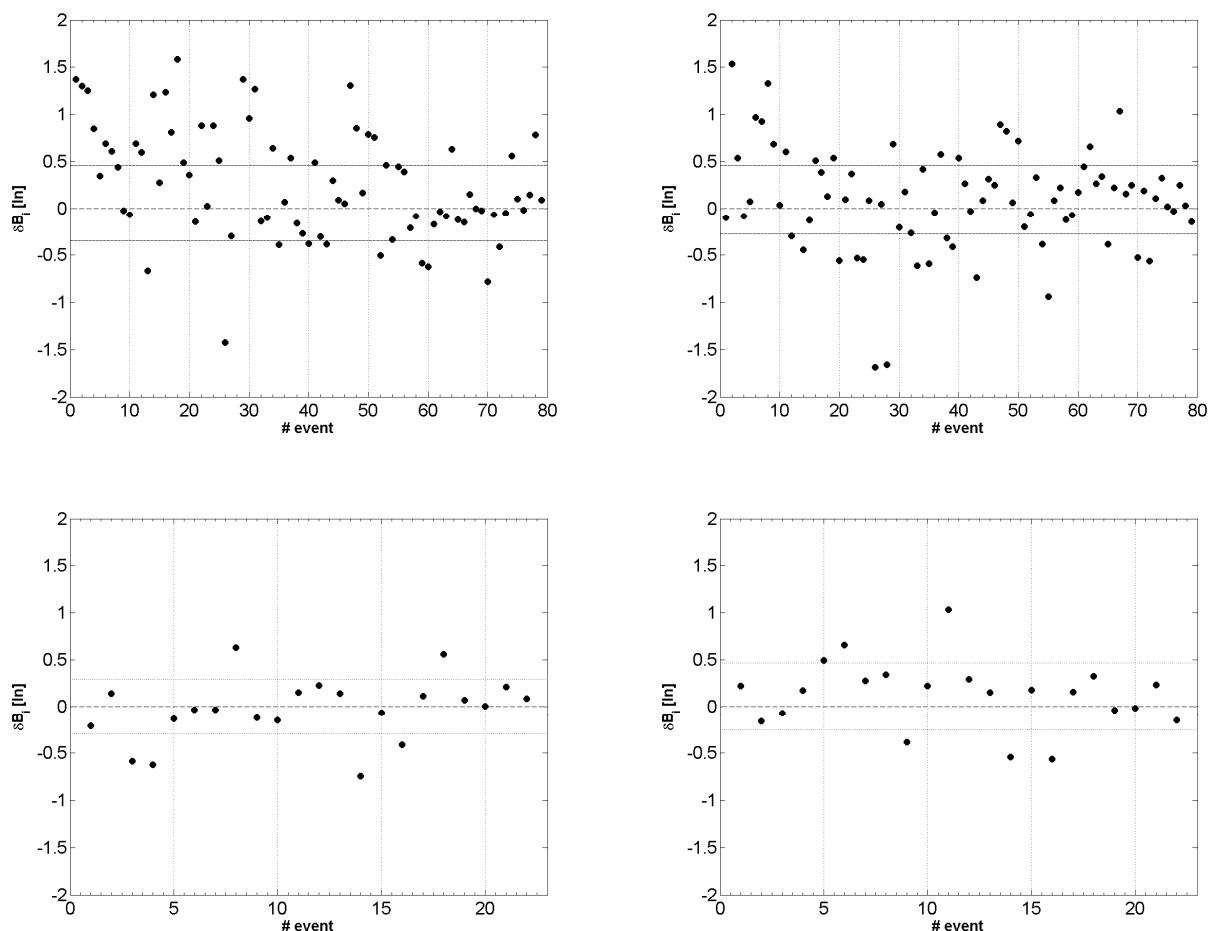

Figure 8. Between event error of DBN2_B (Top) and DBN2_E (bottom) at T = 0.1s (left) and T = 2.0s (right).

The spatial distributions of the between-event terms of DBN2_B periods are reported in Figure 9, in which the circles in green/orange indicate that the predictions are, on average, lower/higher than the observations. As expected, the 1976-1977 Friuli events are generally underestimated while the 2012 events are, on average, well reproduced by the DBN2_GMPEs, especially at long periods.
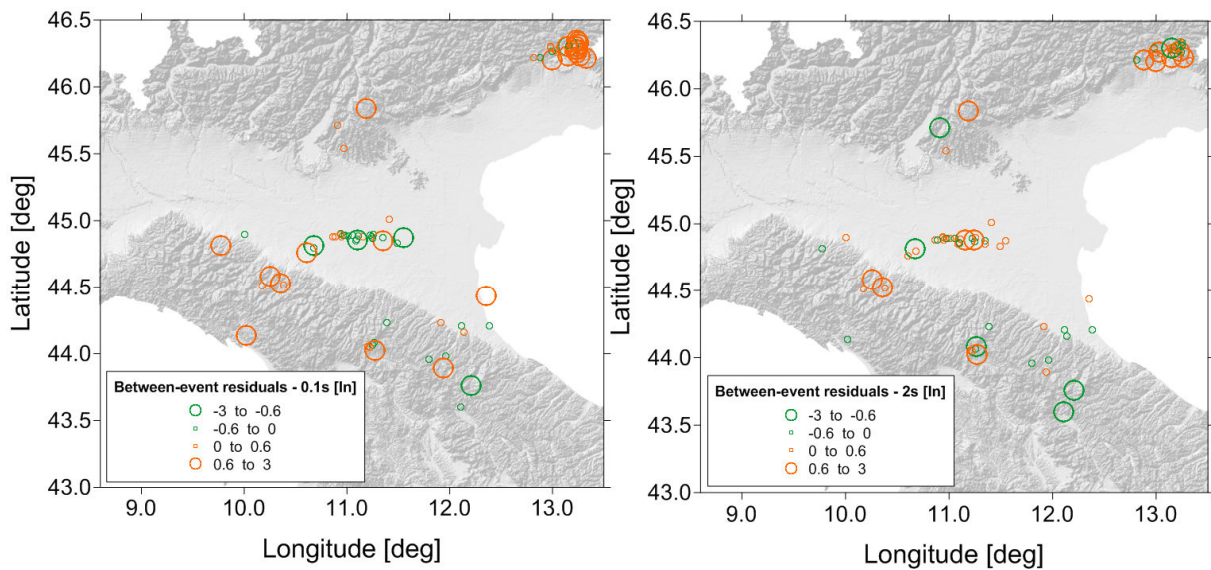

Figure 9. Between-event residuals spatial distributions of DBN2_B at T = 0.1s (left) and T = 2.0s (right).

	Research and Development Program on Seismic Ground Motion	**Ref : SIGMA-2014-D2-133** **Version : 02**
edf cea AREVA Enel Σigma L'ENERGIA CHE TI ASCOLTA. Seismic Ground Motion Assessment	CONFIDENTIAL *Restricted to SIGMA scientific partners and members of the consortium, please do not pass around*	**Date :** February 17th 2015 **Page :** 20 / 42

Within-event errors, site terms and event and station corrected terms

Figures 10 and 11 show the within event, the site term and event and site corrected residuals distributions for the two datasets and two periods (T=0.1s and T = 2s). The W_{ij} and $W_{ij,o}$ are plotted in function of distance, while the S2S term as function of the station number, coloured according to the site classes. In annex B, the sites terms for all investigated periods together the corresponding station information are reported.

As already discussed in the previous section, we remark that the two datasets are characterized by site classes that are not uniformly distributed over distance, since C and C1 sites are mainly located in epicentral area and A and B sites are far from the seismic sources. As consequence, the different contribution to the ground motion variability could be not simply isolated. The W_{ij} residuals have amplitude in the range -3/3, comparable to what observed for the total residuals and show similar trends with distance (Figure 6 and 7) both at long and short periods. This results indicate that the event-contribution to the total variability is small and is irrelevant for the distance scaling.

The residuals corrected for the event and site terms ($\delta W_{o,ij}$) strongly decrease in amplitude (range −2/+2 at T = 0.1s) and show very slight dependence on distance and frequency. This results suggest that large part of the variability in the two datasets is relative to the site contribution, mainly due to the classes A and B in the short to medium period range. However, the site responses of classes A and B, the most of them located at epicentral distances larger than 50km, could be also affected by anisotropies in the seismic wave propagation. This point can be highlighted by Figures 12, that shows the spatial distribution of the site terms for the two datasets at T = 0.1s and T = 2s.

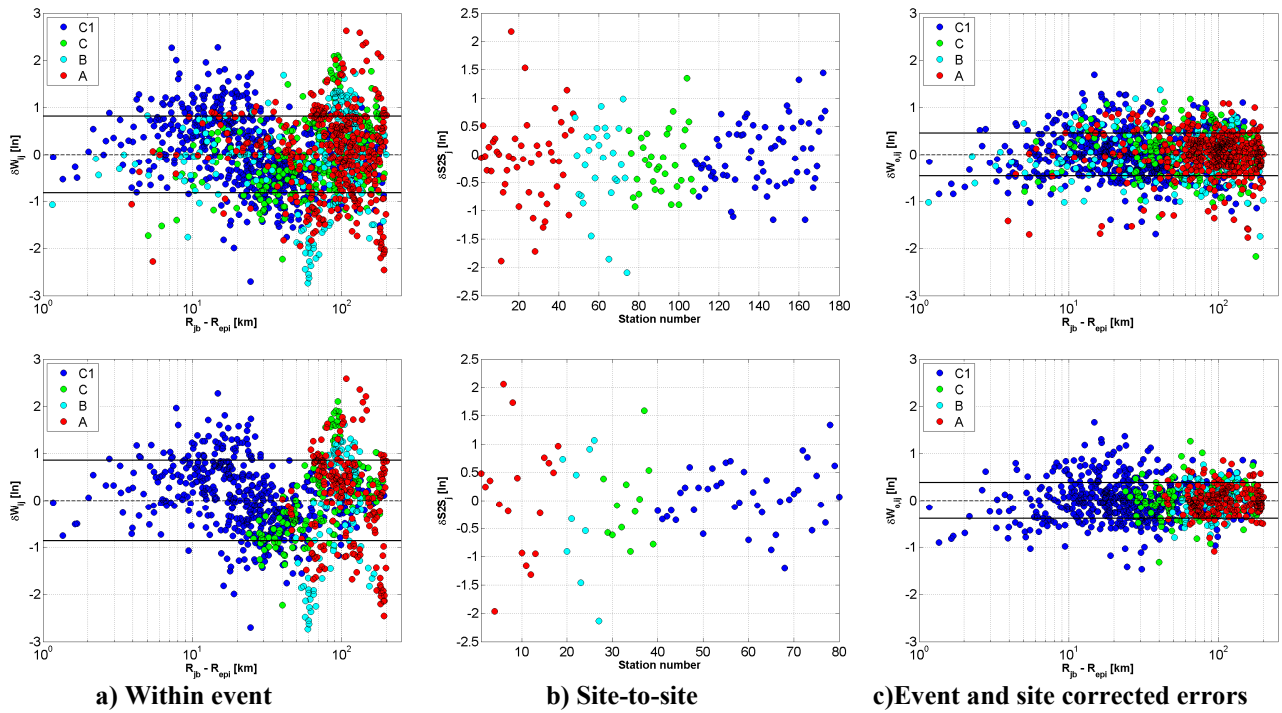|	Research and Development Program on Seismic Ground Motion	Ref : SIGMA-2014-D2-133
		Version : 02
edf cea AREVA Enel Sigma	CONFIDENTIAL *Restricted to SIGMA scientific partners and members of the consortium, please do not pass around*	Date : February 17th 2015 Page : 21 / 42

Figure 10. T = 0.1s: within-event error a); site-to-site variability b); event and site corrected error c). Top: DBN2_B; Bottom: DBN2_E. The residuals are grouped according to the site classifications.
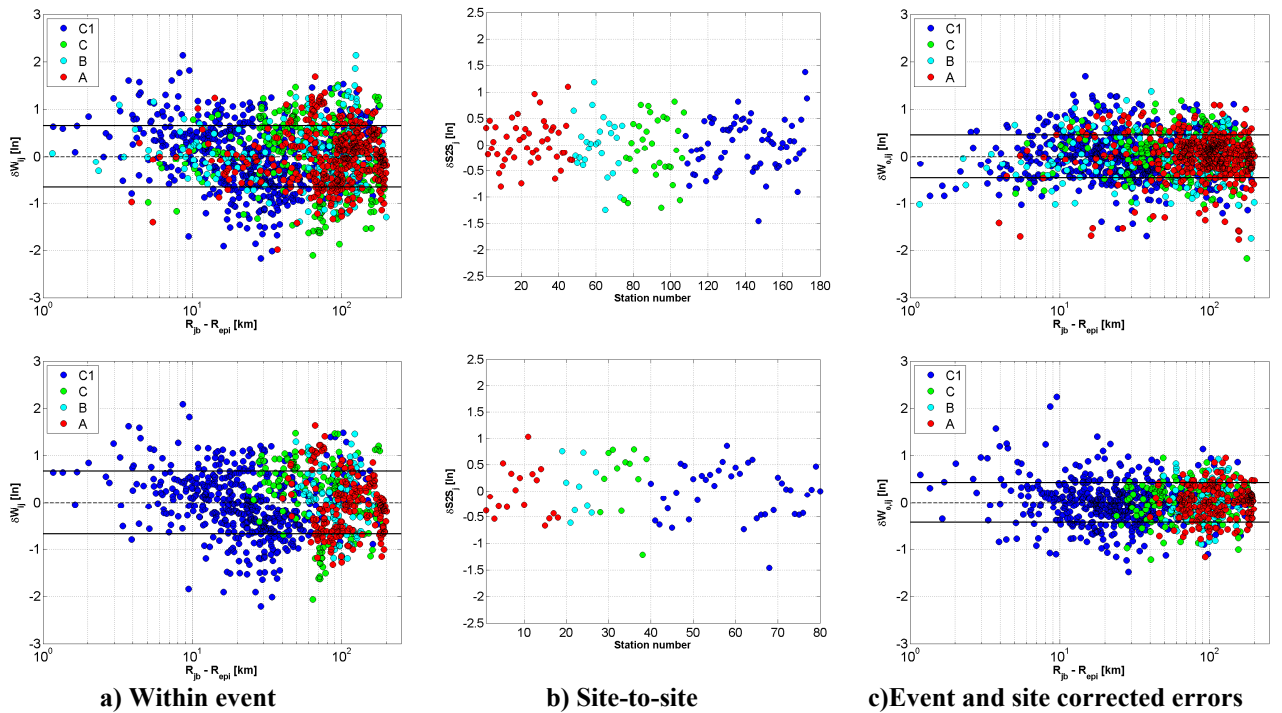
Figure 11. T = 2s: within-event error a); site-to-site variability b); event and site corrected error c). Top: DBN2_B; Bottom: DBN2_E. The residuals are grouped according to the site classifications.

High-frequency amplification and low frequency de-amplification characterize the rock and stiff sites located on the North-eastern sector of the Alps, while the opposite occur for the recording sites located on the Apennines chain. This feature is particular evident in case of DBN2_E dataset, characterized by a single seismogenic source. This large site-variability between northern and southern rock and stiff sites might be also attributed to difference in the regional propagation. In particular, the reflection of the body waves from the Moho could affect the high-frequency ground motion in northern Italy at epicentral distance between 70 and 200km, as observed by various authors (Bragato et al., 2011.
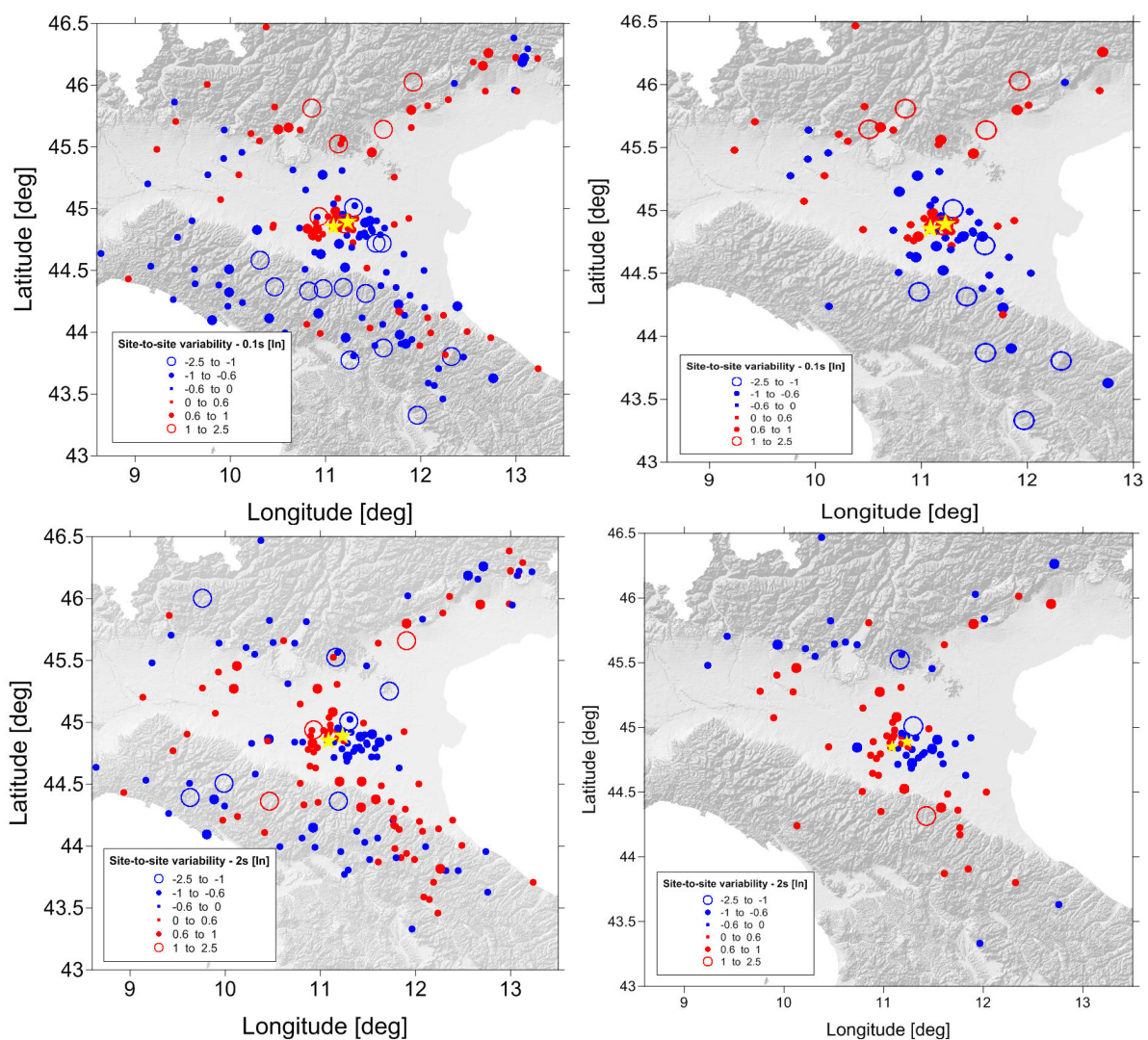

Figure 12. Site to site terms for DBN2_B (left) and DBN2_E (right) at 0.1s (Top) and 2s (Bottom).

Standard deviations

The standard deviations associated to the residual distributions previously discussed are shown in Figure 13 for the two datasets. Following the definitions of Table 1, in the upper panel there are: i) the total standard deviation σ_T; ii) the different components of ground motion variability (between-events sigma τ, and within-event sigma ϕ, see Table 1) and iii) the total single stations standard deviation (σ_{ss}); in the lower panel there are: i) the within-event sigma ϕ; ii) the event and site corrected standard deviation ϕ_{ss} and iii) the site-to-site variability ϕ_{s2s}.
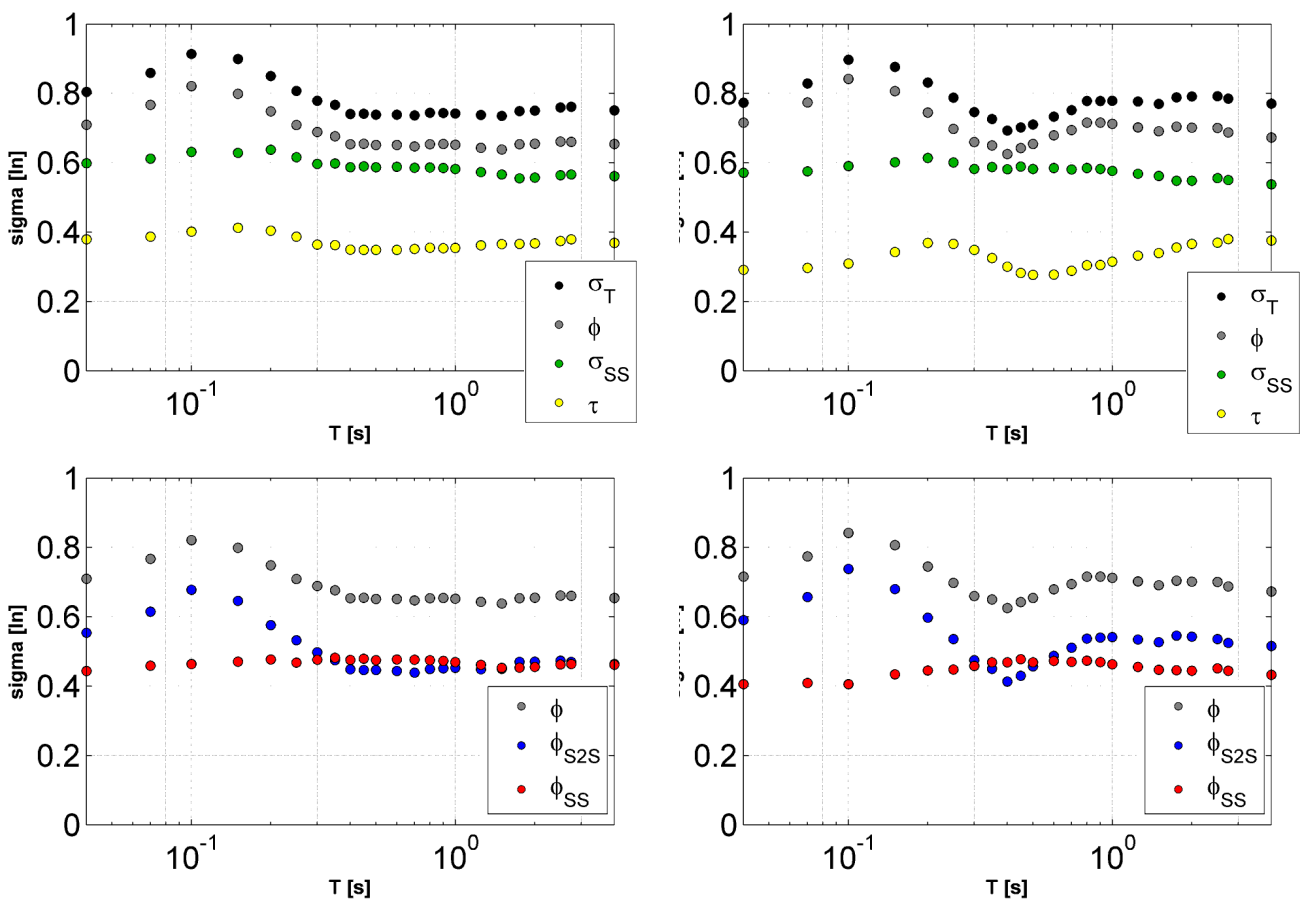

Figure 13. Standard deviation components vs. period for DBN2_B (left) and DBN2_E (right). Standard deviations are expressed in natural logarithms.

No significant differences are observed between the two datasets, in terms of natural logarithms of standard deviation components. The total standard deviation (σ_T) varies between 0.7 and 0.9, with

the largest values observed at short periods (around 0.1s). However, the between-events standard deviation of DBN2_E is smaller than DBN2_B (0.3 against 0.4 at T = 0.1s). Furthermore, the within-event standard deviation trends are quite similar up to 0.3s, while there is an increment of sigma values of DBN2_E around 0.5 - 1s.

The total standard deviations are characterized by a bump centred at 0.1s. Differently from what observed by Boore et al. (2014) for the NGA-West2 GMPEs, this bump is only partially controlled by the τ component and the major contribution is relative to the site-to-site variability. We interpret this large variability at short periods as an effect related to an apparent site effect at rock and stiff sites located on the Alpine chains, caused by the Moho reflections. To test this hypothesis, we evaluate the different component of the variability for a subset extracted from DBN2_E considering the maximum distance up to 100km, in order to exclude the furthest stations. In this case, the total standard deviation is reduced down to 0.73 at T = 0.1

Single station sigma

In this paragraph, we investigate in detail the main features of the event and site corrected standard deviations for all stations and at individual sites. Figure 14 shows the distribution of the single-station sigma at individual sites $\phi_{ss,s}$ for the two datasets. The values of the average single-station sigma ϕ_{ss} as well as the average of sigma associated to the within-event residuals ϕ are also shown.

In comparison to DBN2_B, at short periods the DBN2_E has the lowest average single-station sigma values and the individual values follow a narrower distribution. Since all the records in DBN2_E come from the same seismogenic source, the sampled travel paths cover a restricted azimuthal range with respect to DBN2_E, thus the associated variability is closer to single-station-single-path than single station standard deviation. At longer periods, the two average variability are similar, however the distributions for DBN2_E is skewed, with the tail on the left side shorter than

the right side. This means that the majority of sites is characterized by limited dispersions, but for a small number of stations, the observed ground motion is strongly variable.

All values of single station sigma at all periods are reported in ANNEX_B and ANNEX_C, respectively for the two datasets.
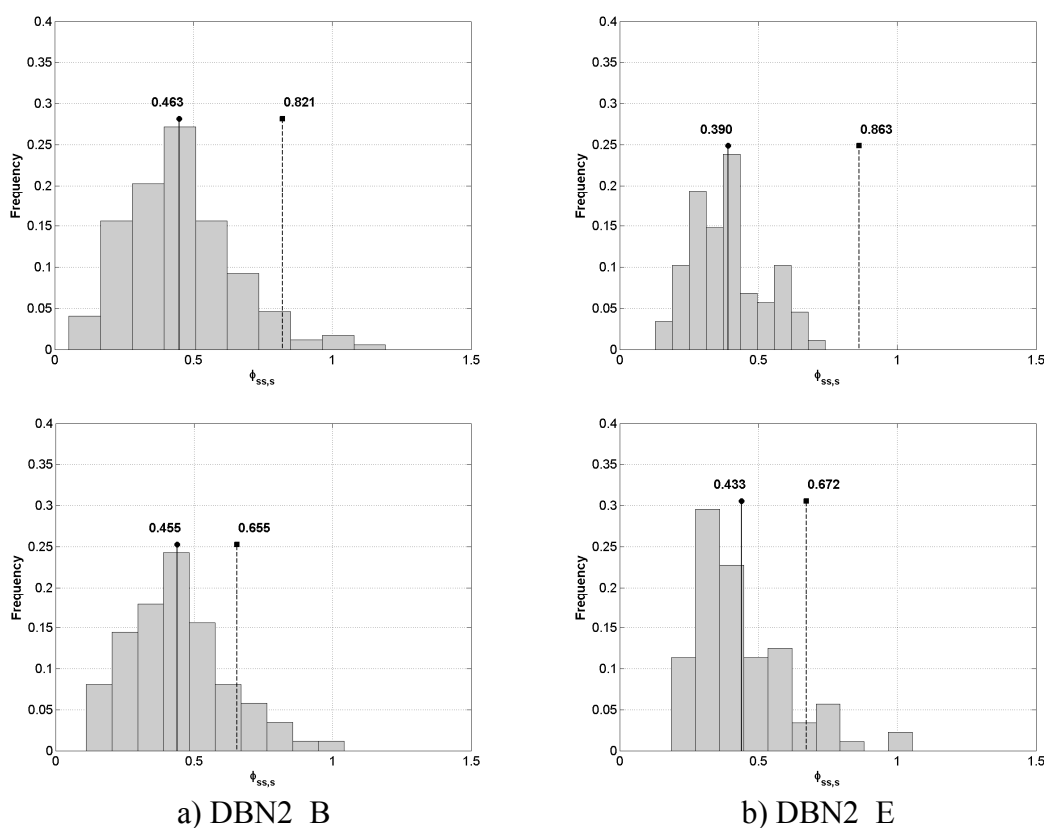

a) DBN2_B   b) DBN2_E

Figure14. Frequency of the single-station standard deviation at individual sites $\phi_{ss,s}$. Top: T = 0.1s; bottom: T = 2.0s; a) DBN2_B, b) DBN2_E. (Continuous line with dot indicates the single station standard deviation; dashed line with square indicates the standard deviation of the within-event error).

Figure 15 and 16 display the single-station sigma for individual sites $\phi_{ss,s}$ obtained from the DBN2_B and DBN2_E at the selected periods. On average, the single-station sigma is around 0.46 (natural log) units for DBN2_B, while it has values ranging from 0.4 to 0.46 for DBN2_E. All the stations with single station sigma larger than 0.7 are labelled in the Figure 14. While at short periods, the largest variability is observed at sites located outside the Po Plain for DBN2_B (Figure

16), at long periods it is observed for the stations in the epicentral area, especially for DBN2_E (stations T08 group, MIR01, SAN0 and FIN0).
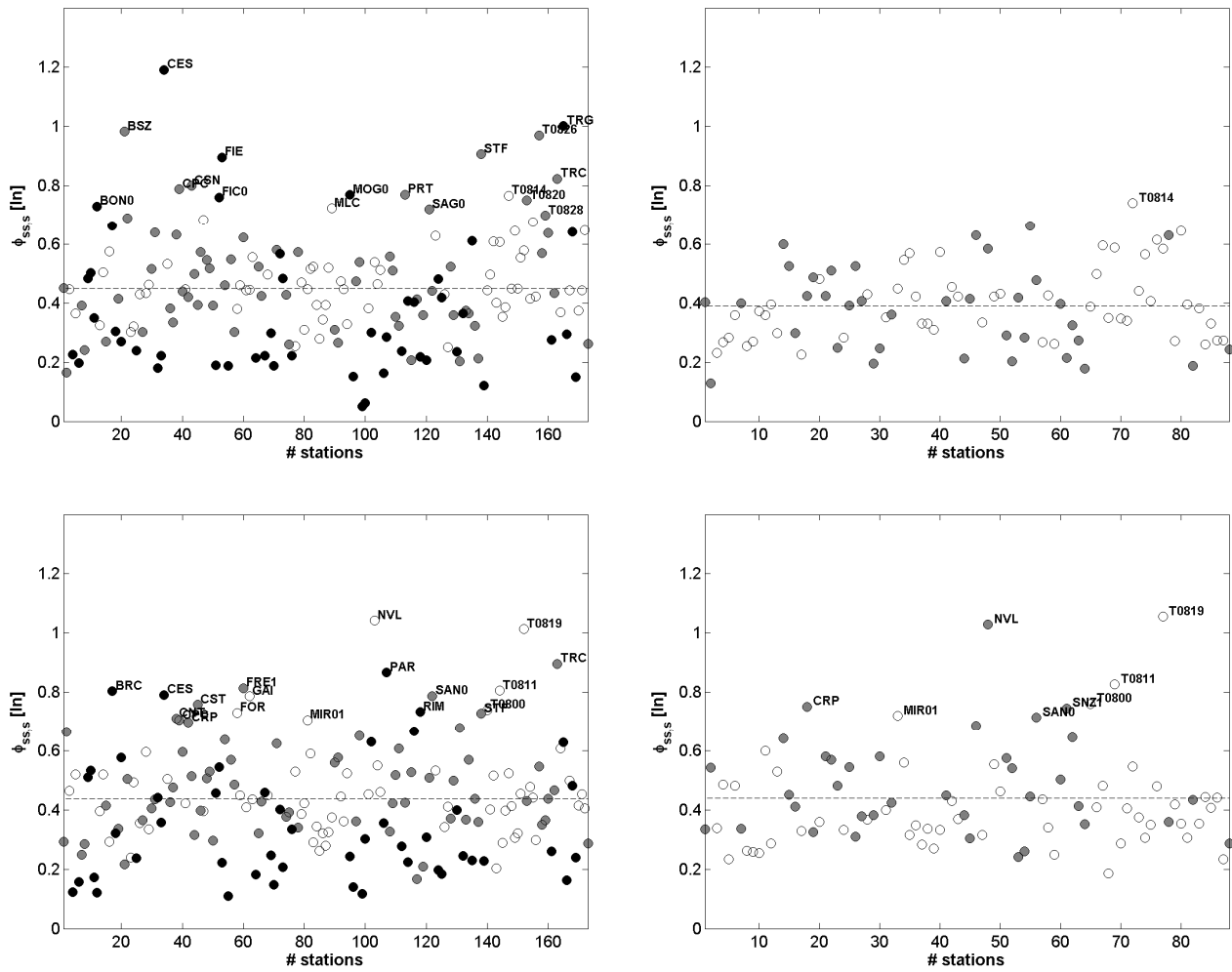

Figure15. Single-station sigma at individual sites $\phi_{ss,s}$ for DBN2_B(left) and DBN2_E (right). Top: T=0.1s; Bottom: T=2s. Black circles: stations with 3-5 records; Grey circles: stations with 6-10 records; White circles: stations with more than 10 records.
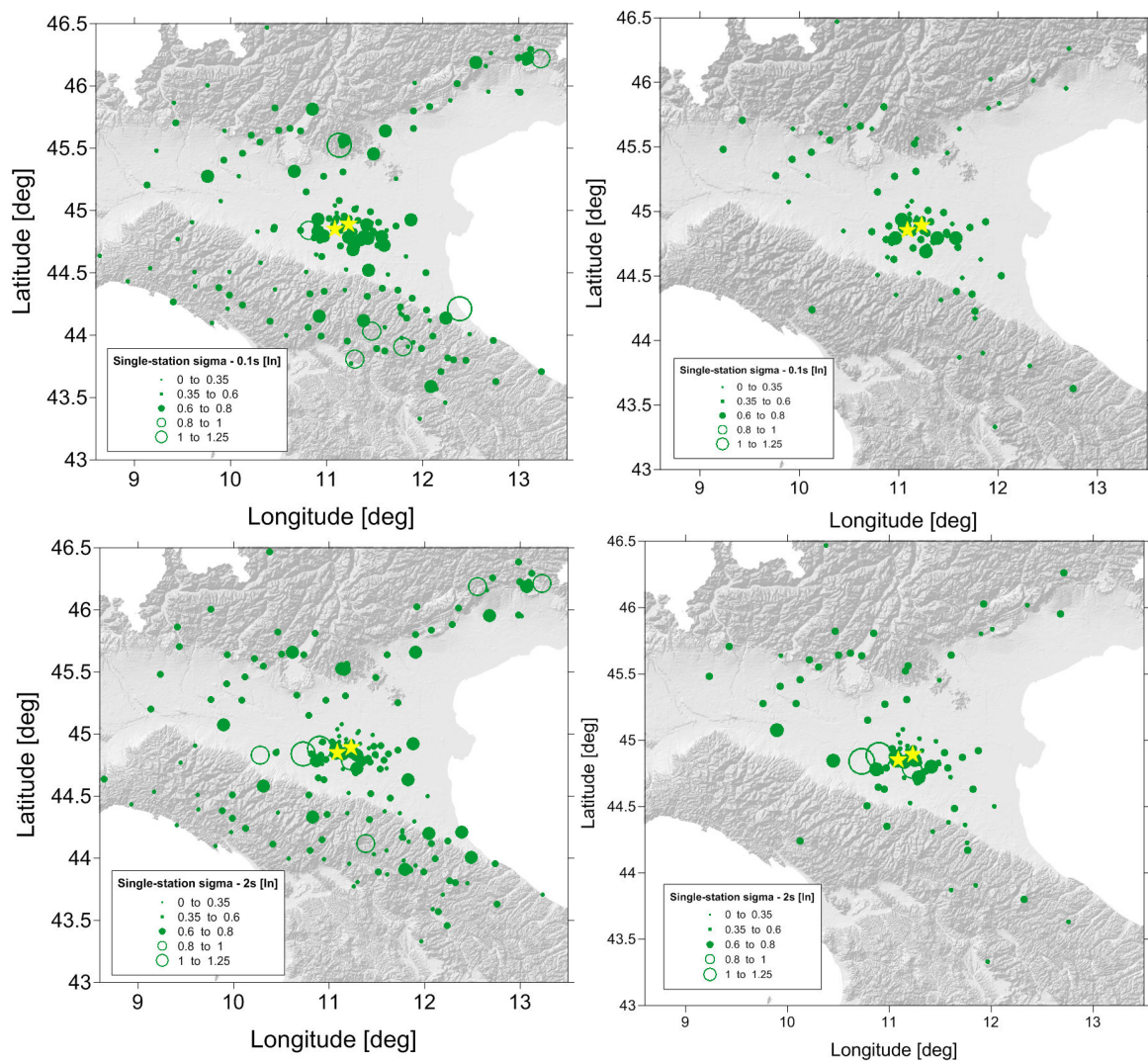
Figure16. Spatial distribution of event corrected standard deviation $\phi_{ss,s}$ for the DBN2_B (left) and DBN2_E (right) datasets. Top: T=0.1s; bottom: T=2s. Yellow stars: mainshocks of the 2012 Emilia sequence.

To highlight the outliers data of DBN2_E, Figure 17 shows the spatial distribution of the event-corrected standard deviations $\phi_{ss,s}$ larger than 0.6 together with the corresponding site term S2S, considering stations with more than 5 records.

The sites with the largest values of sigma are concentrated around the epicentres of the main events both at short and long periods. These stations show small site terms (within -/+ 0.6), in agreement with the assigned class; therefore the observed variability among the ground motions recorded at the

same stations could be related to effects depending on source-observer configuration, such as

forward/backward directivity, distance from the patch slip or presence of velocity pulses.
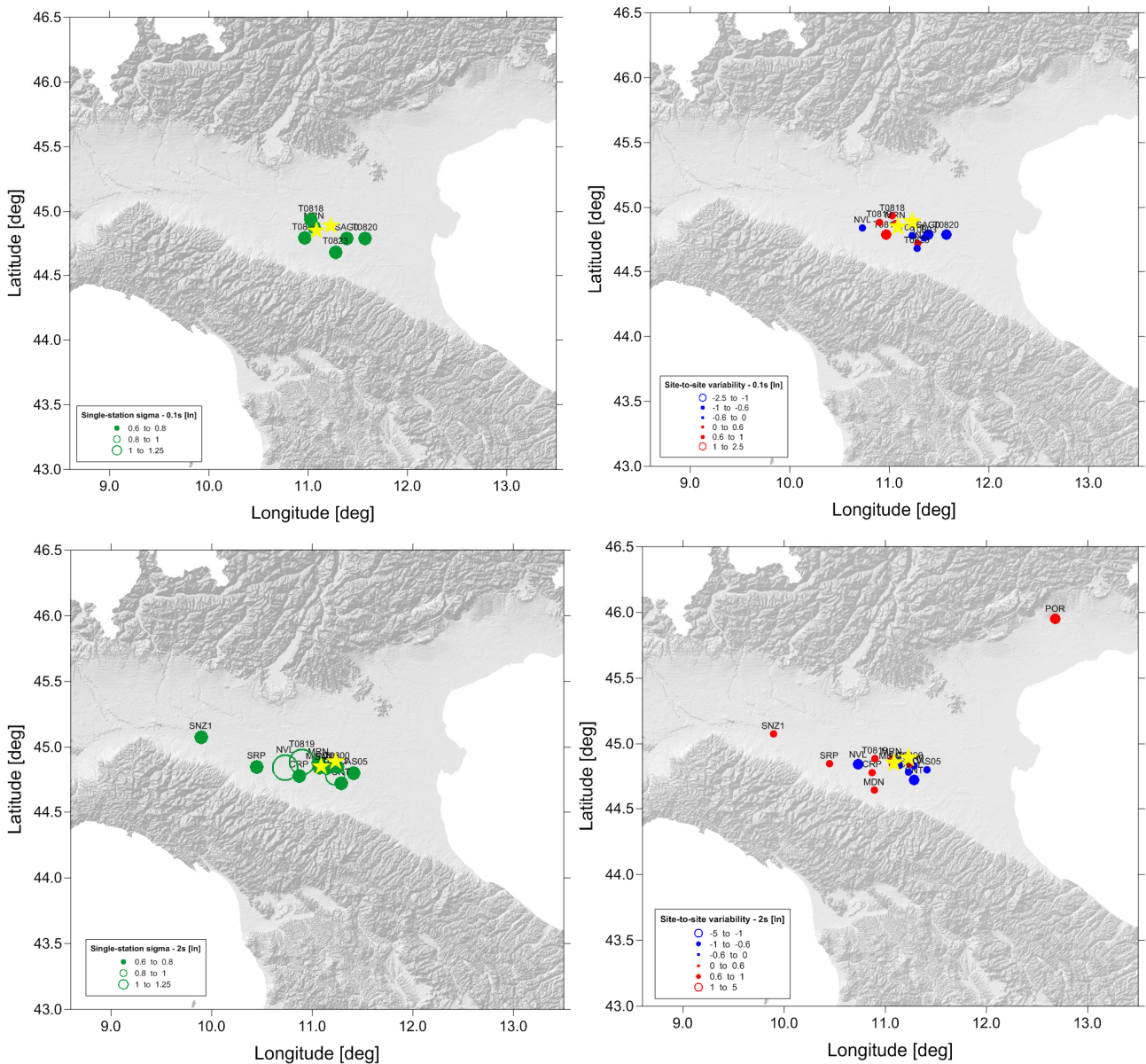

Figure17. Spatial distribution of the stations with event corrected standard deviation higher than 0.6 for the DBN2_E dataset. Left: event corrected standard deviation $\phi_{ss,s}$. Right: corresponding site term S2S. Top: T=0.1s; bottom: T=2s. Yellow stars: mainshocks of the 2012 Emilia sequence.

Figure 18 shows the spatial distribution of the outliers for the site-to-site term S2S, evaluated as

lower than -0.6 or higher than 0.6, with the corresponding single station sigma at individual site.

The stations located in the epicentral area tend to be amplified at short periods, but the associated single station sigma are low. Distant stations located northern and southern to the mainshocks have opposite behaviours, showing high-frequency amplification/de-amplification respectively. This trend is inverted at low frequency. These effects can be related to the complex wave propagation within the Po Plain region that cannot be separated by local site effects.
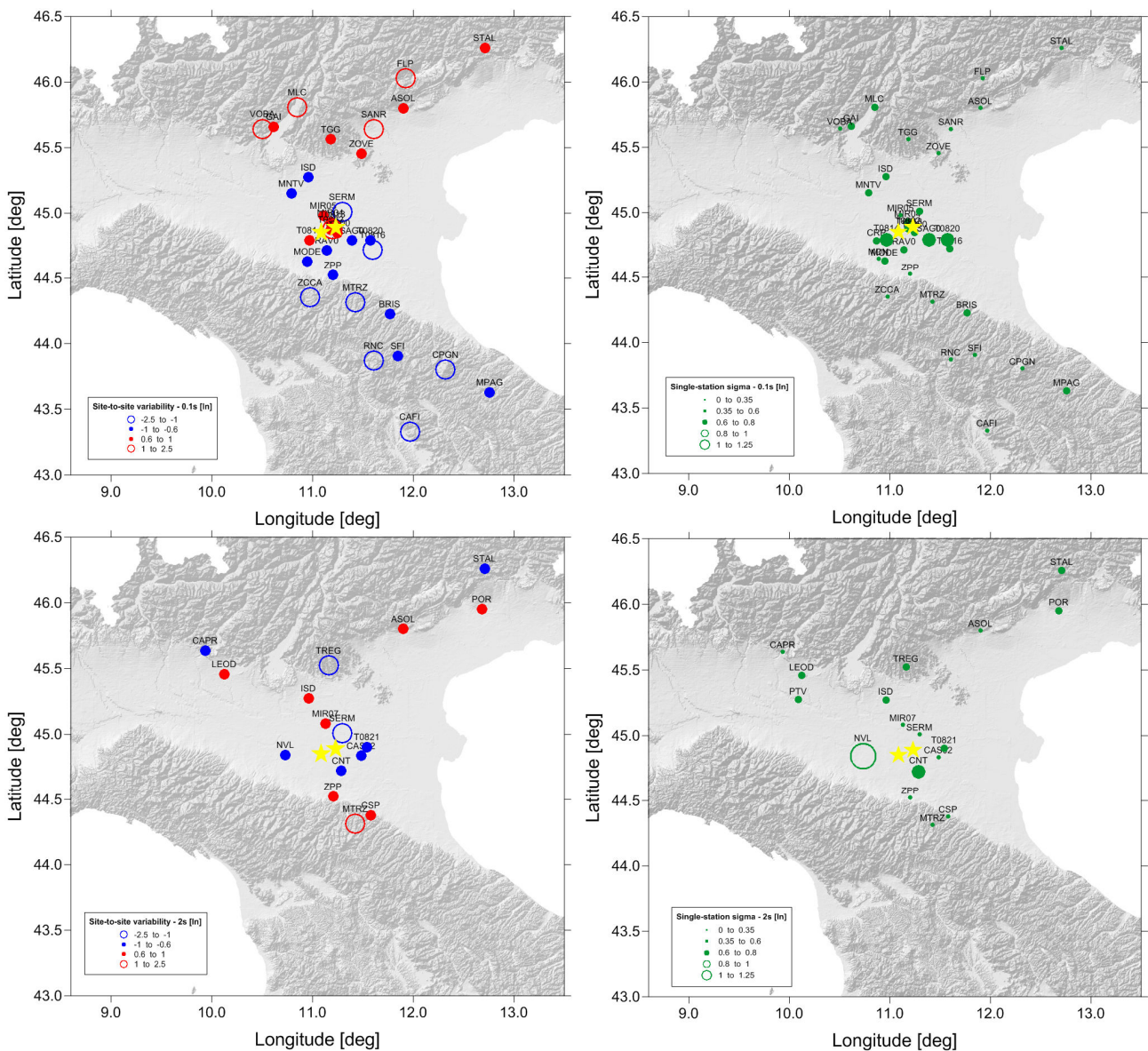

Figure 18. Spatial distribution of the stations with site term less than -0.25 or higher than 0.25 for the DBN2_E dataset. Left: site term S2S. Right: corresponding event corrected standard deviation $\phi_{ss,s}$. Top: T=0.1s; bottom: T=2s. Yellow stars: mainshocks of the 2012 Emilia sequence.

	Research and Development Program on Seismic Ground Motion	Ref : SIGMA-2014-D2-133 Version : 02
		Date : February 17[th]2015 Page :30 / 42
	CONFIDENTIAL *Restricted to SIGMA scientific partners and members of the consortium, please do not pass around*	

Single station sigma at representative sites

We also investigate the variability at all stations. Here we discuss only some selected stations, shown in Figure 19. The single-station standard deviation ($\phi_{ss,s}$) and the site term (S2S) are plotted against the period in Figure 20 and 21. All the plots are reported in ANNEX_D.
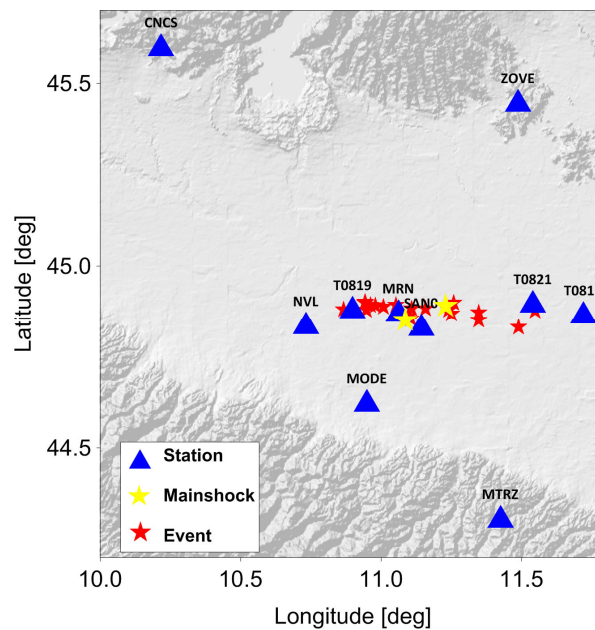
Figure 19. Location of the investigated sites (Blue triangles). Star represents the epicentres of the 2012 Emilia seismic sequence.

Figure 20 shows 4 stations which recorded in the far field the Emilia sequence, located to north and south of the epicentres, respectively. On average, the single station sigma $\phi_{ss,s}$ is around 0.4, with larger values for CNCS (up to 0.68) and smaller ones for MTRZ (lower than 0.3). When we also include other events than the Emilia sequence (DBN2_B case), the variability increases at short periods for CNCS and ZOVE, related to the contribution of different paths, while the site terms remain similar. The southern stations (MODE C1 and MTRZ B*) show slightly small single station sigma (~ 0.35 units) and have opposite site term behaviour with respect to the northern sites.

Figure 21shows the stations located in the epicentral area (NVL, T0819, SAN0, MRN, T0821 and T0815 all in C1).These sites have site terms almost null, while the single station sigma is higher

than 0.5 for sites located over the epicentres and around 0.3 for the furthest stations (T0821 and T0815). This result indicates a GMPEs-coherent site classification, but a very large variability occurs at sites located close the seismogenic source.

To highlight this feature in the middle panel of Figure 20, for each station, the within residuals are plotted with different colors depending on the PGA values.

The dispersions among the residuals is very large for the sites over the epicentres, but no clear dependence on the intensity ground motion can be found. At long periods, the largest errors are in correspondence of the maximum PGA (T0819 and SAN0). On the other hand, the short period residuals can be lower than the mean for the highest PGA (i.e. MRN). This suggests that a cause of variability among records can be related to the occurrence of non-linear site effects, that actually are not included in the GMPEs used in the analysis.
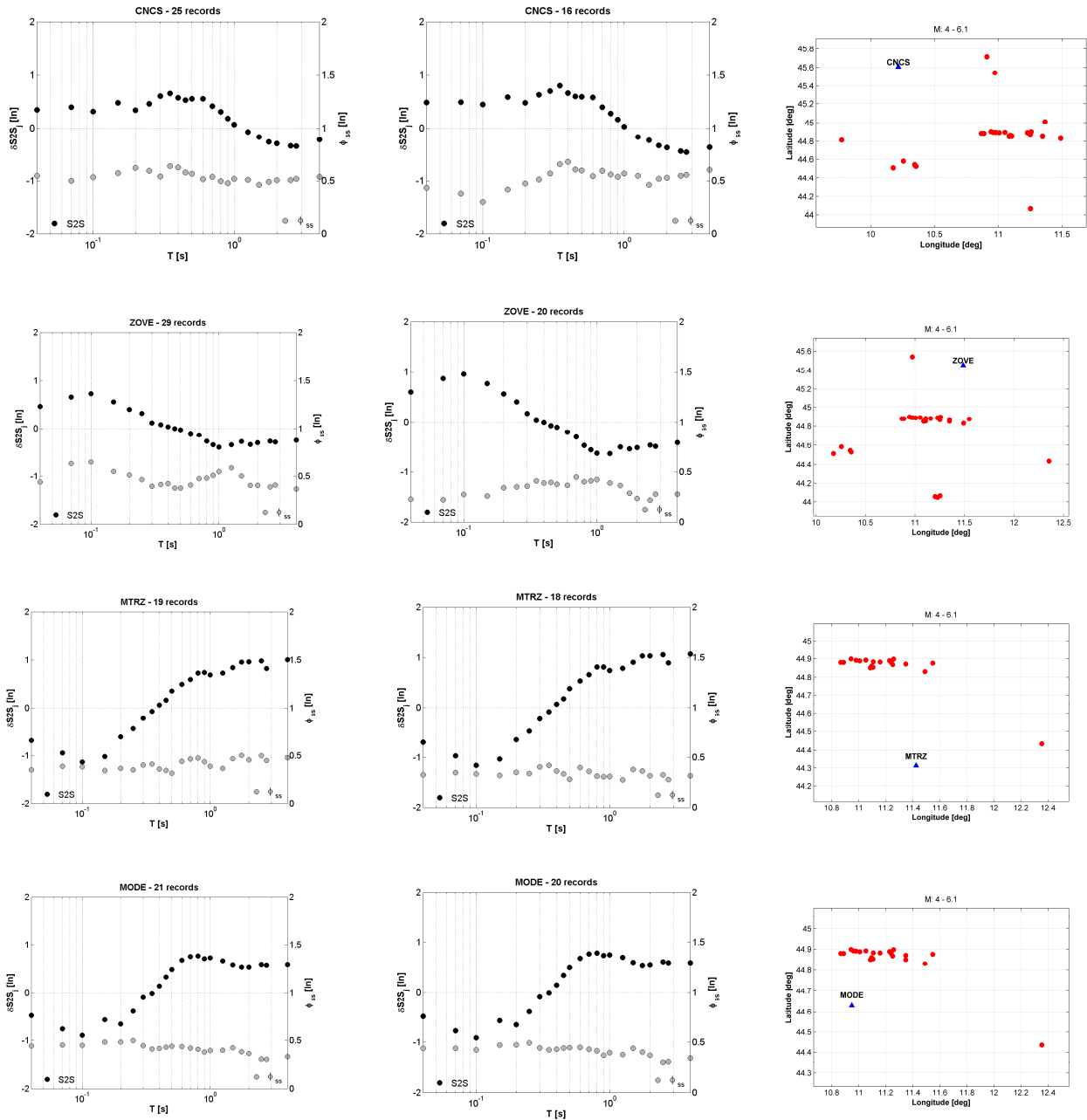
	Research and Development Program on Seismic Ground Motion	Ref : SIGMA-2014-D2-133
EDF cea AREVA Enel L'ENERGIA CHE TI ASCOLTA. sigma Seismic Ground Motion Assessment		Version : 02
	CONFIDENTIAL *Restricted to SIGMA scientific partners and members of the consortium, please do not pass around*	Date : February 17th 2015 Page : 32 / 42

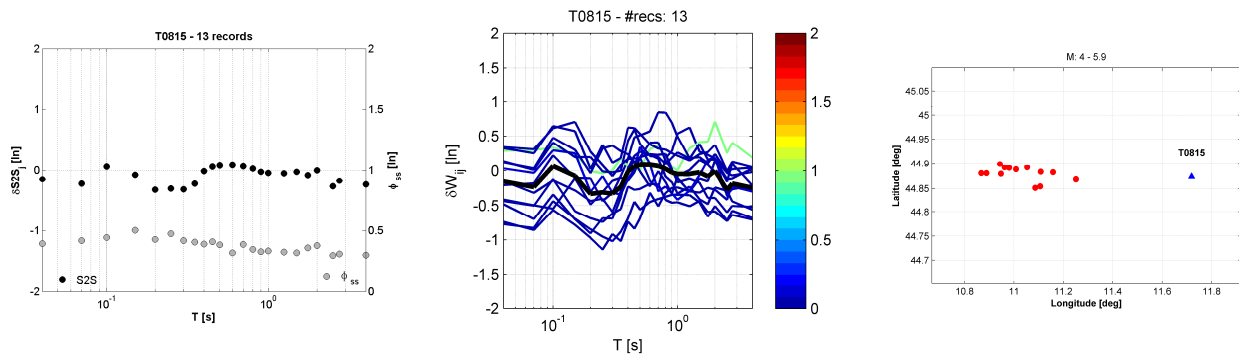**Figure 20.** Site error (black circles) and single station sigma (grey circles) for DBN2_E far source selected stations (left). Location of station (blue triangle) and recorded events (red circles) (right)

	Research and Development Program on Seismic Ground Motion	Ref : SIGMA-2014-D2-133
EDF CEA AREVA Enel Sigma		Version : 02
	CONFIDENTIAL *Restricted to SIGMA scientific partners and members of the consortium, please do not pass around*	Date : February 17th 2015 Page : 33 / 42

	Research and Development Program on Seismic Ground Motion	**Ref : SIGMA-2014-D2-133** **Version : 02**
edf cea AREVA Enel Σigma Seismic Ground Motion Assessment L'ENERGIA CHE TI ASCOLTA.	**CONFIDENTIAL** *Restricted to SIGMA scientific partners and members of the consortium, please do not pass around*	**Date :** February 17th 2015 **Page :** 34 / 42
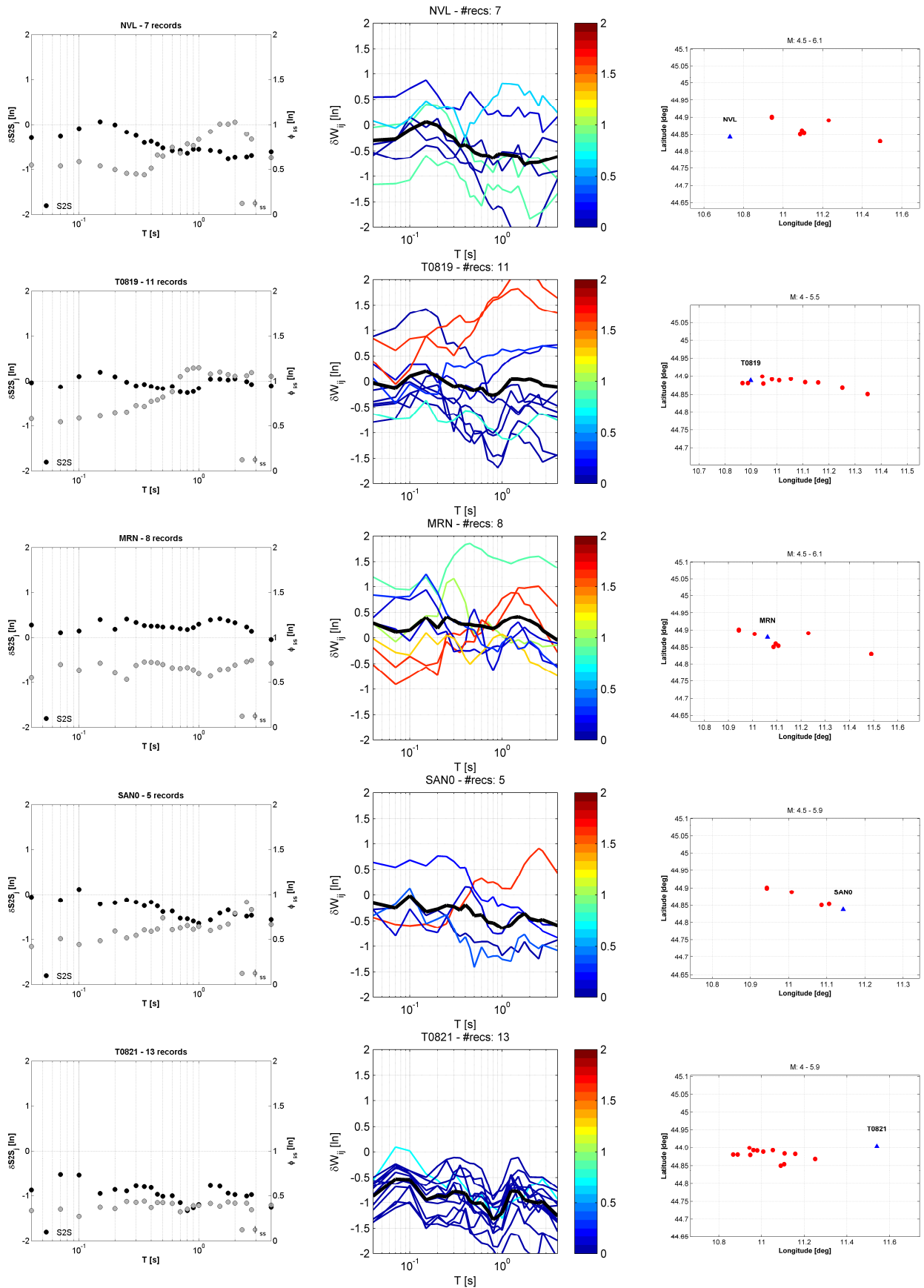
Figure 21. Site error (black circles) and single station sigma (grey circles) for DBN2_E selected stations in the epicentral area (left). Location of station (blue triangle) and recorded events (red circles) (right).

5. DISCUSSIONS AND CONCLUSIONS

In this report we explored the ground motion variability at single sites for the Po Plain region. The total standard deviation (σ_T) has been decomposed into different components (between event τ, site-to-site ϕ_{S2S} and event and site corrected ϕ_{ss} variability).

Two datasets are analysed: DBN2_B has been compiled and employed by Pacor et al. (2013) in the first stages of the project with the aim of producing regional GMPEs for Northern Italy (1539 records, 79 events, 173 stations); DBN2_E is an extraction of DBN2_B in a smallest spatial area and temporal window in order to include only events related to the 2012 Emilia sequence (715 records, 22 events, 68 stations). The results are here discussed for two selected periods (short period T=0.1s and long period T=2s).

Figure 22 shows the values of single station sigma ϕ_{ss} for northern Italy, compared with those by other studies. In particular we consider the standard deviations obtained by Luzi et al. (2014) for the Italian datasets: i) BIea, used to derive the most recent GMPEs for Italy (Bindi et al. 2011) (829 records, 146 events, 117 stations);ii) BIea2, which enlarges BIea, including all records from magnitude 4 (2805 records from 658 events and 254 stations) events; iii) L'Aquila dataset (ABR) composed by records related to the 2009 L'Aquila sequence, in order to isolate one seismic source

(401 records, 41 events, 38 stations). Furthermore, we also consider the standard deviations computed by the models proposed by Rodriguez-Marek et al. (2013) using data from California, Japan, Switzerland, Taiwan, and Turkey. The authors developed a magnitude-dependent (MKM), a distance dependent (MKR),and a magnitude- and distance-dependent model (MKC).
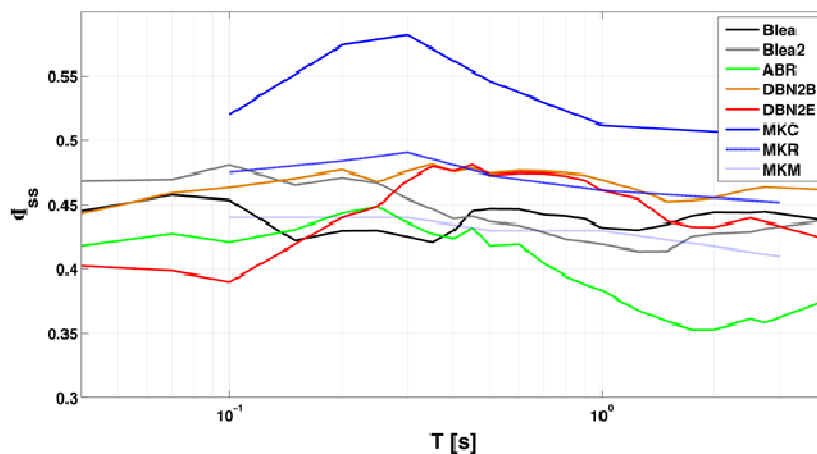

Figure 22. Single-station standard deviation (ϕss) obtained from different studies. MKR is evaluated for R = 20Km, MKM for M = 6 mad MKC for M=6 and R 20Km)

No strong variation is observed among the single station sigma from different studies (except MKC model): on average, almost all are in the range 0.4 – 0.48. The estimates obtained for single-source conditions, i.e DBN2_E and ABR), provide the lowest values at short and long periods, respectively.

In Figure 23, the total single stations sigma are plotted for the Italian datasets (DBN2_B, DBN2_E ABR, BIea2 and BIea), showing that, as expected, the regional datasets provide the lowest total single stations sigma in comparison to the national ones, as the event contributions are largest when different source and focal mechanisms are considered.

	Research and Development Program on Seismic Ground Motion	Ref : SIGMA-2014-D2-133
		Version : 02
edf cea AREVA Enel Σigma	CONFIDENTIAL _Restricted to SIGMA scientific partners and members of the consortium, please do not pass around_	Date : February 17[th]2015 Page :36 / 42
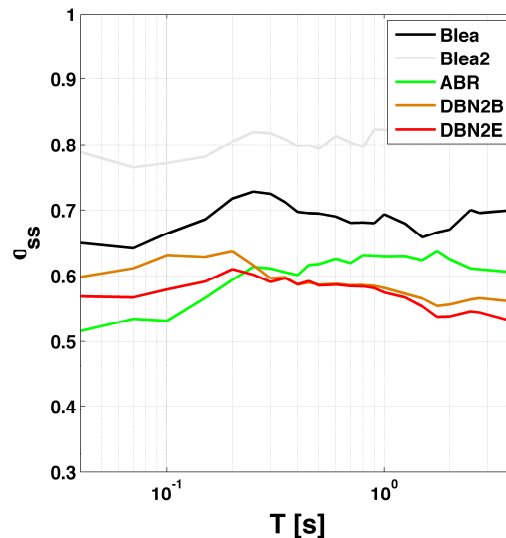
Figure 23. Total single-station sigma (σ_{ss}) relative to different Italian datasets.

The main conclusions of this study are the following:

1) The general trend of standard deviation components (vs. period) for both datasets (DBN2_B and DBN2_E) is quite similar, we only observe a small reduction of the event-variability and the event and site corrected variability at high frequency for DBN2_E with respect to DBN2_B (Figure 13). The lower standard deviations at short periods for DBNE_E can be related to consider a single seismogenic source and a narrow azimuth range of travel paths.

2) In both cases, the total standard deviation (σ_T) is about 0.8 (Figure 13) and decreases to about 0.58 when the ergodic assumption is removed (σ_{ss}); for both datasets the largest values are around T= 0.1s, that we interpret as partially due to the an effect related to an apparent site effect at rock and stiff sites located on the Alpine chains, caused by the Moho reflections.

3) The event and site corrected sigma computed for Northern Italy is generally comparable to the values inferred for national dataset (BIea in Figure 22 and the models derived by Rodriguez-Marek et al., 2013); the total single stations sigma is lower for the regional dataset (ABR and DBN2_B and DBN2_E in Figure 23)

4) The outlier stations has been identified according two different criteria for DBN2_E: i) event and site corrected standard deviation larger than 0.6; ii) site term smaller than -0.6 and larger than 0.6. The selected stations generally are not the same: we observe that in case of high values of site term ($\delta S2S_i$), the corresponding single station sigma is small ($\phi_{ss,s}$), and viceversa.

5) The sites with the largest values of $\phi_{ss,s}$ are concentrated around the two Emilia mainshocks, and the observed variability can be probably related to source effects; stations located northern and southern to the mainshocks have opposite behaviours in terms of site amplification. It can be probably due to the complex wave propagation within the Po Plain.

References

Al Atik, L., Abrahamson, N. A., Bommer, J. J., Scherbaum, F., Cotton, F. and Kuehn,N. (2010). The Variability of Ground-Motion Prediction Models and Its Components, Seismol. Res. Lett., 81(5), 794–801, doi:10.1785/gssrl.81.5.794.

Bindi, D., Pacor, F., Luzi, L., Puglia, R., Massa, M., Ameri, G., & Paolucci, R. (2011). Ground motion prediction equations derived from the Italian strong motion database. Bulletin of Earthquake Engineering, 9(6), 1899-1920.

Boore D.M., Stewart J.P., Seyhan E., Atkinson J.M. (2014). NGA-West2 Equations for Predicting PGA, PGV, and 5% Damped PSA for Shallow Crustal Earthquakes. Earthquake Spectra, 30(3), 1057-1085.

Bragato P.L., Sugan M., Augliera P., Massa M., Vuan A., Saraò A. (2011). Moho reflection effects in the Po Plain (Northern Italy) observed from instrumental and intensity data. Bulletin of the Seismological Society of America, vol. 101(5), 2142-2152.

CEN, European Committee for Standardization (2003).Eurocode 8: design provisions for earthquake resistance of structures, Part 1.1: general rules, seismic actions and rules for buildings, prEN 1998-1.

Luzi L., Pacor F., Ameri G., Puglia R., Burrato P., Massa M, Augliera P., Franceschina G., Lovati S., Castro R. (2013). Overview on the strong-motion data recorded during the May-June 2012 Emilia seismic sequence Seismological Research Letters, 84(4), 629-644.

Luzi L., Bindi D., Puglia R., Pacor F. and Oth A. (2014). Single-Station Sigma for Italian Strong-Motion Stations. Bulletin of the Seismological Society of America, 104(1), 467-483.

Pacor F., Luzi L., Massa M., Bindi D. (2012). Ranking of available GMPEs from residual analysis for northen Italy and definition of reference GMPEs. SIGMA Project, Deliverable SIGMA-2012-D2-53-02.

Pacor F., Luzi L., D'Amico M., Puglia R. and Bindi D. (2013). Updating and analysis of strong-motion database of Northern Italy through the residual analysis between empirical predictions and observations in the Po plain region. SIGMA ENEL Project, Deliverable SIGMA 0002-2013

Paolucci, R., Pacor, F., Puglia, R., Ameri, G., Cauzzi, C. and Massa, M. (2011). Record processing in ITACA, the new Italian strong-motion database, in Earthquake Data in Engineering Seismology. Predictive Models, Data Management and Networks, S. Akkar, P. Gulkan and T. Van Eck (Editors), Geotechnical, Geological and Earthquake Engineering series, 14(8), 99-113.

Rodriguez-Marek, A., G. A. Montalva, F. Cotton, and F. Bonilla (2011), Analysis of Single-Station Standard Deviation Using the KiK-net Data, Bull. Seismol. Soc. Am., 101(3), 1242–1258, doi:10.1785/0120100252

Rodriguez-Marek, A., Cotton, F., Abrahamson, N.A., Akkar, S., Al Atik, L., Edwards, B., Montalva, G.A. and Dawood H.M. (2013). A Model for Single-Station Standard Deviation Using Data from Various Tectonic Regions. Bulletin of Seismological Society of America. 103(6), 3149-3163.

Scasserra G., Stewart J. P., Bazzurro P., Lanzo G., and F. Mollaioli (2009). A Comparison of NGA Ground-Motion Prediction Equations to Italian Data, Bull. Seismol. Soc. Am., 99, 5, 2961–2978, doi: 10.1785/0120080133.

	Research and Development Program on Seismic Ground Motion	Ref : SIGMA-2014-D2-133
		Version : 02
	CONFIDENTIAL *Restricted to SIGMA scientific partners and members of the consortium, please do not pass around*	Date : February 17th 2015 Page :39 / 42

ANNEX A

Event metadata and between event residuals

ANNEX_A.xlsx

ANNEX B

Station metadata and single-station sigma

ANNEX_B.xlsx

ANNEX C

Station metadata and site-to-site variability

ANNEX_C.xlsx

ANNEX D

- Single-station sigma and site error of DBN2_E.
  - Location of stations and recorded events.

ANNEX_D.pdf